A COMPUTATIONALLY EFFICIENT PWM ALGORITHM FOR MULTILEVEL INVERTERS

T.G. Subhash Joshi A.S. Haneesh
subhash@erdcitvm.org haneesh@erdcitvm.org
Power Electronics Group, Centre for Development of Advanced Computing,
(Erstwhile ER&DCI), Trivandrum – 695 033

G. Narayanan V.T. Ranganathan
gnar@ieee.org vtran@ee.iisc.ernet.in
Department of Electrical Engineering,
Indian Institute of Science, Bangalore – 560 012

Abstract

Centred space vector PWM (CSVPWM) technique is popularly used for three level voltage source inverters. The reference voltage vector is synthesized by time-averaging of the three nearest voltage vectors produced by the inverter. Identifying the three voltage vectors, and calculation of the dwelling time for each vector are both computationally intensive. This paper analyses the process of PWM generation in CSVPWM. This analysis breaks up a three-level inverter into six different conceptual two level inverters in different regions of the fundamental cycle. Control of 3-level inverter is viewed as the control of the appropriate 2-level inverter. The analysis leads to a systematic simplification of the computations involved, finally resulting in a computationally efficient PWM algorithm. This algorithm exploits the equivalence between triangle comparison and space vector approaches to PWM generation. This algorithm does not involve any 3-phase/2-phase or 2-phase/3-phase transformation. This also does not involve any transformation from rectangular to polar coordinates, and *vice versa*. Further no evaluation of trigonometric functions is necessary. This algorithm also provides for the mitigation of DC neutral point unbalance, and is well suited to digital implementation. Simulation and experimental results are presented.

1. Introduction

Multilevel neutral point clamped inverters are increasingly used in medium and high power applications [1-3].

Among several PWM techniques for a three-level inverter, centred space vector PWM (CSVPWM) is very popular due to low harmonic distortion in the output waveform [1-2]. However, the calculations involved are computationally intensive [2].

Considerable efforts have been made to simplify these calculations [2]. Towards further simplification, the process of PWM generation involved in CSVPWM is analyzed here. The analysis leads to a systematic simplification of the method of calculation, resulting in a computationally efficient PWM algorithm.

2. Three-level voltage source inverter

A three-level voltage source inverter is shown in Fig. 1. Every leg of the inverter is a single-pole, triple-throw switch. The inverter has 3^3 or 27 switching states, and produces 18 active voltage vectors and one zero vector as shown in Fig. 2.

Active vectors $\mathbf{V_1}$, $\mathbf{V_2}$, … $\mathbf{V_6}$ are termed here as 'pivot vectors.' While all other active vectors are produced by a unique inverter state, a pivot vector is produced by two inverter states as shown in Fig. 2. The inverter states that produce a pivot vector are termed 'pivot states.' The dwell time of a pivot vector is equally divided between the two pivot

states in centred space vector PWM, which is explained in the following section.

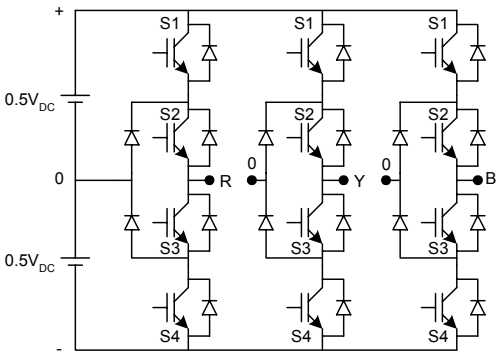

Fig. 1 Schematic of a three-level voltage source inverter

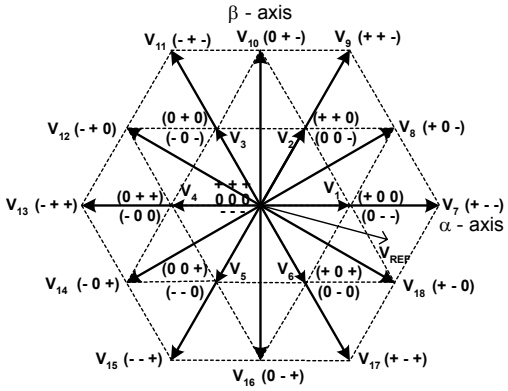

Fig. 2 Switching states and voltage vectors of a three-level inverter
V_1 - V_6 are pivot vectors

3. Centred space vector PWM

Centred space vector PWM involves different stages of calculation in every subcycle or sampling period as shown in Fig. 3.

Given three-phase sinusoidal modulating waves (v_R, v_Y, v_B), 3-phase to 2-phase transformation is carried out as given in (1). The two-phase voltage reference is then transformed from rectangular to polar coordinates in the stationary reference frame as shown in (2).

$$v_\alpha = \frac{3}{2} v_R ; \qquad v_\beta = \frac{\sqrt{3}}{2}(v_Y - v_B) \qquad ...(1)$$

$$V_{REF} = \sqrt{(v_\alpha^2 + v_\beta^2)}, \qquad \theta = \tan^{-1}\frac{v_\beta}{v_\alpha} \qquad ...(2)$$

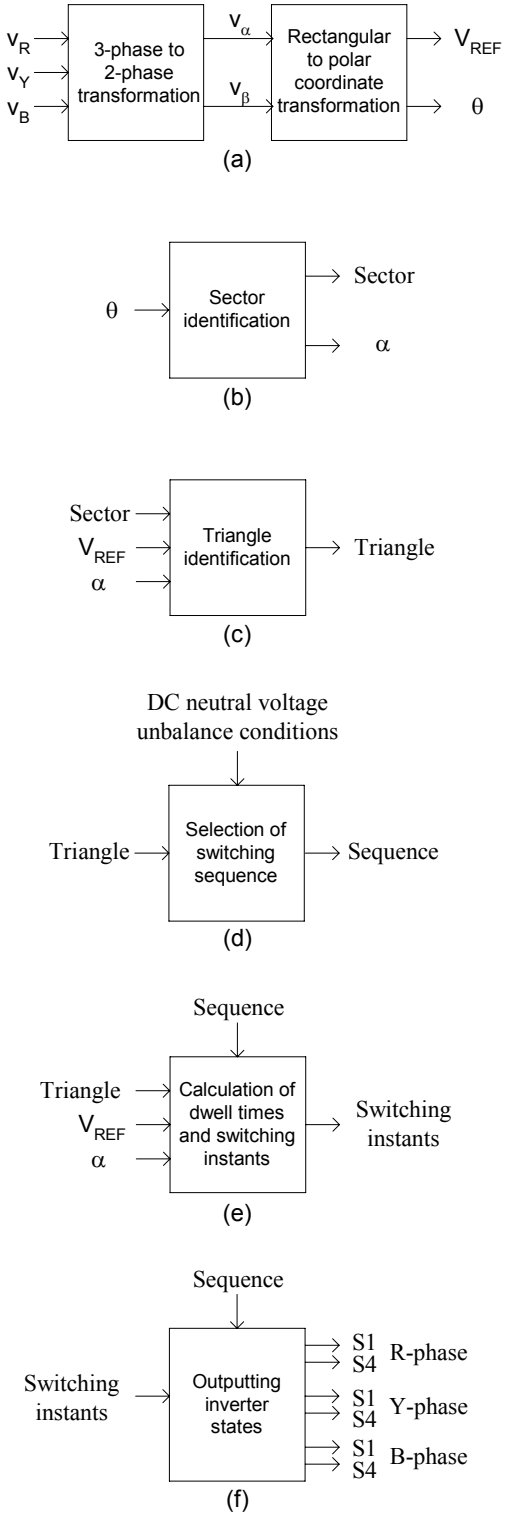

Fig. 3 Stages of calculation in centred space vector PWM

TABLE I: SECTOR IDENTIFICATION

Range of θ	Sector
0^o – 60^o	1
60^o – 120^o	2
120^o – 180^o	3
180^o – 240^o	4
240^o – 300^o	5
300^o – 360^o	6

TABLE II: BOUNDARIES OF TRIANGLES IN A SECTOR

Common side of triangles	Mathematical description
T1 and T3	$V_{B1}(\alpha)=\frac{\sqrt{3}}{4\cos(30^o-\alpha)},\ 0^o \le \alpha < 60^o$ ...(4*a*)
T2 and T3	$V_{B2}(\alpha)=\frac{\sqrt{3}}{4\sin(60^o-\alpha)},\ 0^o \le \alpha < 30^o$ ...(4*b*)
T3 and T4	$V_{B3}(\alpha)=\frac{\sqrt{3}}{4\sin(\alpha)},\quad 30^o \le \alpha < 60^o$ ...(4*c*)

TABLE III: IDENTIFICATION OF TRIANGLE AND CALCULATION OF DWELL TIMES

Triangle	Condition(s)	Dwell times for the three voltage vectors
T1	$V_{REF} \le V_{B1}(\alpha),$ $0^o \le \alpha < 60^o$	$T_1=2V_{REF}\frac{\sin(60^o-\alpha)}{\sin(60^o)}T_S$ $T_2=2V_{REF}\frac{\sin(\alpha)}{\sin(60^o)}T_S$ $T_Z=T_S-T_1-T_2$ ...(5*a*)
T2	$V_{REF} > V_{B2}(\alpha),$ $0^o \le \alpha < 30^o$	$T_7=\left[2V_{REF}\frac{\sin(60^o-\alpha)}{\sin(60^o)}-1\right]T_S$ $T_8=2V_{REF}\frac{\sin(\alpha)}{\sin(60^o)}T_S$ $T_1=T_S-T_7-T_8$ ...(5*b*)
T3	$V_{B1}(\alpha) < V_{REF} \le V_{B2}(\alpha),$ *if* $0^o \le \alpha < 30^o$ $V_{B1}(\alpha) < V_{REF} \le V_{B3}(\alpha),$ *if* $30^o \le \alpha < 60^o$	$T_1=\left[1-2V_{REF}\frac{\sin(\alpha)}{\sin(60^o)}\right]T_S$ $T_2=\left[1-2V_{REF}\frac{\sin(60^o-\alpha)}{\sin(60^o)}\right]T_S$ $T_8=T_S-T_1-T_2$ ...(5*c*)
T4	$V_{REF} > V_{B3}(\alpha),$ $30^o \le \alpha < 60^o$	$T_8=2V_{REF}\frac{\sin(60^o-\alpha)}{\sin(60^o)}T_S$ $T_9=\left[2V_{REF}\frac{\sin(\alpha)}{\sin(60^o)}-1\right]T_S$ $T_2=T_S-T_8-T_9$ ...(5*d*)

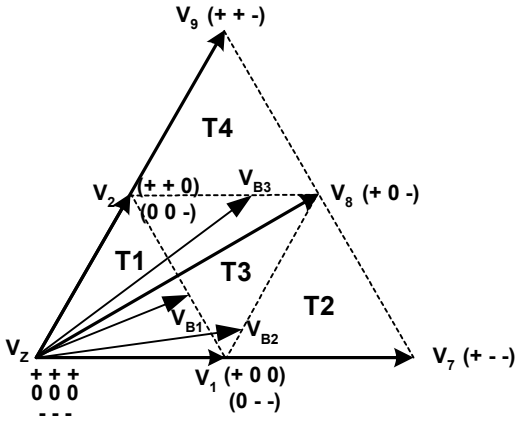

Fig. 4 Triangles in sector 1

The sector, in which the reference vector falls, can be identified using θ as shown in Table I. If sector = n, then

$$\alpha=\theta-(n-1)60^o \quad ...(3)$$

Sector 1 is spatially divided into four triangles – T1, T2, T3 and T4 – as shown in Fig. 4. The inter-triangular boundaries in a sector are described mathematically by (4) in Table II.

When the reference vector is in sector 1, its tip may fall in one of the triangles T1, T2, T3 or T4. The triangle in which it falls can be identified using the conditions given in Table III. Note that this requires evaluation of $V_{B1}(\alpha)$, $V_{B2}(\alpha)$ and $V_{B3}(\alpha)$, which are trigonometric functions of α as seen from Table II.

The reference vector is synthesized by time-averaging of the three vectors, whose tips form the vertices of the given triangle, e.g. $\mathbf{V_1}$, $\mathbf{V_7}$ and $\mathbf{V_8}$ for triangle T2.

The pivot vector for T2 is $\mathbf{V_1}$, and that for T4 is $\mathbf{V_2}$ as shown in Table IV. For T1 and T3, both $\mathbf{V_1}$ and $\mathbf{V_2}$ are possible pivot vectors. Correspondingly, there is a choice in switching sequences also as shown in Table IV.

The choice of the pivot vector and sequences has a bearing on the DC neutral point unbalance. For a given direction of power flow, say from the DC bus to the three-phase load, one of the above two choices leads to charging of the top capacitor and discharging of the bottom capacitor. The other choice of pivot vector and sequences leads to charging of the bottom capacitor and discharging

of the top capacitor. Appropriate choice is made depending on DC neutral unbalance, if any [2].

TABLE IV: PIVOT VECTORS AND SWITCHING SEQUENCES IN SECTOR 1

Triangle	Pivot vector	Switching sequence	
		Clockwise sequence	Counterclockwise sequence
T1	$\mathbf{V_1}$(+00, 0--)	(+00, 000, 00-, 0--)	(0--, 00-, 000, +00)
	$\mathbf{V_2}$(++0, 00-)	(++0, +00, 000, 00-)	(00-, 000, +00, ++0)
T2	$\mathbf{V_1}$(+00, 0--)	(+00, +0-, +--, 0--)	(0--, +--, +0-, +00)
T3	$\mathbf{V_1}$(+00, 0--)	(0--, 00-, +0-, +00)	(+00, +0-, 00-, 0--)
	$\mathbf{V_2}$(++0, 00-)	(00-, +0-, +00, ++0)	(++0, +00, +0-, 00-)
T4	$\mathbf{V_2}$(++0, 00-)	(++0, ++-, +0-, 00-)	(00-, +0-, ++-, ++0)

The dwell times of the three voltage vectors are calculated as shown in Table III [1]. Note that the four triangles have different sets of formulae to calculate the dwell times.

Clockwise and counterclockwise sequences are used in alternate subcycles. With the dwell times of the three vectors and the switching sequence known, the switching instants can be calculated.

The inverter state is changed appropriately at every switching instant. The gating signals of the devices are changed appropriately. Table V shows the relationship between the inverter states and the gating signals of the individual devices for all possible states in sector 1.

TABLE V: INVERTER STATES AND GATING SIGNALS

Inverter state	R-phase		Y-phase		B-phase	
	S1	S4	S1	S4	S1	S4
---	0	1	0	1	0	1
000	0	0	0	0	0	0
+++	1	0	1	0	1	0
+00	1	0	0	0	0	0
0--	0	0	0	1	0	1
++0	1	0	1	0	0	0
00-	0	0	0	0	0	1
+--	1	0	0	1	0	1
+0-	1	0	0	0	0	1
++-	1	0	1	0	0	1
	$S2 = \overline{S4},\ S3 = \overline{S1}$		$S2 = \overline{S4},\ S3 = \overline{S1}$		$S2 = \overline{S4},\ S3 = \overline{S1}$	

From the foregoing discussion, the following steps in the CSVPWM algorithm can be identified to be computationally intensive:

(i) Selection of three voltage vectors or identification of triangle in a sector (due to the need for evaluation of trigonometric functions).
(ii) Calculation of dwell times (due to different formulae for the four triangles in a sector).
(iii) Calculation of dwell times in any triangle (since trigonometric functions must be evaluated).
(iv) Three-phase to two-phase transformation of the voltage reference.
(v) Rectangular to polar coordinate transformation of the voltage reference vector.

4. Conceptual two-level inverter

In most PWM techniques in general, and in CSVPWM in particular, a phase switches only between the positive DC bus and the DC bus neutral during the positive half cycle, and only between the DC bus neutral and the negative DC bus during the negative half cycle. This divides the fundamental cycle into six equal regions wherein a three-level inverter essentially acts as a two-level inverter.

There are six such conceptual two-level inverters corresponding to the six regions of the fundamental cycle. The six pivot vectors of the three-level inverter become the zero vectors of these six two-level inverters. The voltage vectors of the conceptual two-level inverter, whose zero vector is the pivot vector $\mathbf{V_1}$, are shown in Fig. 5.

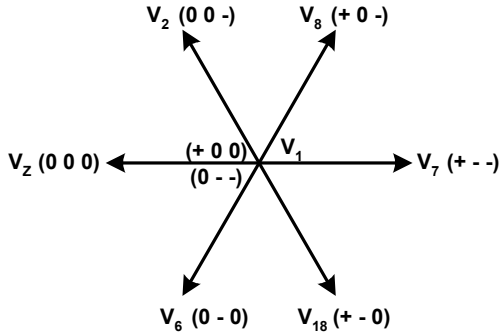

Fig. 5 Voltage vectors produced by a conceptual two-level inverter

5. Steps towards simplification

The computationally intensive steps are considered one-by-one, and simplification is

attempted. Viewing the three-level inverter as a conceptual two-level inverter for the purpose of control proves helpful here.

5.1. Identification of triangle

Assuming that the reference for the three-level inverter is available in the form $V_{REF}\angle\theta$, the nearest pivot vector can be identified using θ as shown in Table VI. The nearest pivot vector is subtracted from the reference vector of the three-level inverter to obtain the reference vector $V^*_{REF}\angle\alpha^*$ corresponding to the conceptual two-level inverter. The angle α^* indicates the triangle in which the tip of the reference vector lies. Thus, the triangle is now identified easily as a sector of the conceptual two-level inverter.

TABLE VI: IDENTIFICATION OF THE NEAREST PIVOT VECTOR USING θ

Range of θ	Nearest pivot vector ($\mathbf{V_{PN}}$)			
	Symbol	In polar coordinates	In rectangular coordinates	As a 3-phase quantity
330° – 30°	$\mathbf{V_1}$	$0.5\angle 0^O$	$\frac{1}{2}+j0$	$\left(\frac{1}{3},\frac{-1}{6},\frac{-1}{6}\right)$
30° – 90°	$\mathbf{V_2}$	$0.5\angle 60^O$	$\frac{1}{4}+j\frac{\sqrt{3}}{4}$	$\left(\frac{1}{6},\frac{1}{6},\frac{-1}{3}\right)$
90° – 150°	$\mathbf{V_3}$	$0.5\angle 120^O$	$-\frac{1}{4}+j\frac{\sqrt{3}}{4}$	$\left(\frac{-1}{6},\frac{1}{3},\frac{-1}{6}\right)$
150° – 210°	$\mathbf{V_4}$	$0.5\angle 180^O$	$\frac{1}{2}+j0$	$\left(\frac{-1}{3},\frac{1}{6},\frac{1}{6}\right)$
210° – 270°	$\mathbf{V_5}$	$0.5\angle 240^O$	$-\frac{1}{4}-j\frac{\sqrt{3}}{4}$	$\left(\frac{-1}{6},\frac{-1}{6},\frac{1}{3}\right)$
270° – 330°	$\mathbf{V_6}$	$0.5\angle 300^O$	$\frac{1}{4}-j\frac{\sqrt{3}}{4}$	$\left(\frac{1}{6},\frac{-1}{3},\frac{1}{6}\right)$

5.2. General formulae for all triangles

The dwell times for the three vectors can be calculated using $V^*_{REF}\angle\alpha^*$ as shown in (6). The formulae are now identical for all triangles or sectors of the two-level inverter.

$$T_X = V^*_{REF}\frac{\sin(60^o-\alpha^*)}{\sin(60^o)}T_S$$

$$T_Y = V^*_{REF}\frac{\sin(\alpha^*)}{\sin(60^o)}T_S$$

$$T_Z = T_S - T_X - T_Y \qquad ...(6)$$

5.3. Avoiding coordinate transformations

The pivot vectors can be expressed as three-phase quantities as shown in the last column of Table VI. The nearest pivot vector can be identified using 3-phase sinusoidal references based on the conditions shown in Table VII. Subtracting the nearest pivot vector from (v_R, v_Y, v_B) as shown in (7) gives the tentative three-phase reference for the two-level inverter.

$$\left(v^*_{RN}, v^*_{YN}, v^*_{BN}\right)=\left(v_R, v_Y, v_B\right)-\left(v_{PNR}, v_{PNY}, v_{PNB}\right) \quad ...(7)$$

TABLE VII: NEAREST AND SECOND POSSIBLE PIVOT VECTORS

Conditions	Nearest pivot vector ($\mathbf{V_{PN}}$)	Condition	Second possible pivot vector
$\lvert v_R\rvert=\max(\lvert v_R\rvert,\lvert v_Y\rvert,\lvert v_B\rvert)$, $v_R>0$	$\mathbf{V_1}$	$v^*_{RN}=\max(v_R,v_Y,v_B)$	–
		$v^*_{YN}=\max(v_R,v_Y,v_B)$	$\mathbf{V_2}$
		$v^*_{BN}=\max(v_R,v_Y,v_B)$	$\mathbf{V_6}$
$\lvert v_B\rvert=\max(\lvert v_R\rvert,\lvert v_Y\rvert,\lvert v_B\rvert)$, $v_B<0$	$\mathbf{V_2}$	$v^*_{RN}=\min(v_R,v_Y,v_B)$	$\mathbf{V_3}$
		$v^*_{YN}=\min(v_R,v_Y,v_B)$	$\mathbf{V_1}$
		$v^*_{BN}=\min(v_R,v_Y,v_B)$	–
$\lvert v_Y\rvert=\max(\lvert v_R\rvert,\lvert v_Y\rvert,\lvert v_B\rvert)$, $v_Y>0$	$\mathbf{V_3}$	$v^*_{RN}=\max(v_R,v_Y,v_B)$	$\mathbf{V_2}$
		$v^*_{YN}=\max(v_R,v_Y,v_B)$	–
		$v^*_{BN}=\max(v_R,v_Y,v_B)$	$\mathbf{V_4}$
$\lvert v_R\rvert=\max(\lvert v_R\rvert,\lvert v_Y\rvert,\lvert v_B\rvert)$, $v_R<0$	$\mathbf{V_4}$	$v^*_{RN}=\min(v_R,v_Y,v_B)$	–
		$v^*_{YN}=\min(v_R,v_Y,v_B)$	$\mathbf{V_5}$
		$v^*_{BN}=\min(v_R,v_Y,v_B)$	$\mathbf{V_3}$
$\lvert v_B\rvert=\max(\lvert v_R\rvert,\lvert v_Y\rvert,\lvert v_B\rvert)$, $v_B>0$	$\mathbf{V_5}$	$v^*_{RN}=\max(v_R,v_Y,v_B)$	$\mathbf{V_6}$
		$v^*_{YN}=\max(v_R,v_Y,v_B)$	$\mathbf{V_4}$
		$v^*_{BN}=\max(v_R,v_Y,v_B)$	–
$\lvert v_Y\rvert=\max(\lvert v_R\rvert,\lvert v_Y\rvert,\lvert v_B\rvert)$, $v_Y<0$	$\mathbf{V_6}$	$v^*_{RN}=\min(v_R,v_Y,v_B)$	–
		$v^*_{YN}=\min(v_R,v_Y,v_B)$	$\mathbf{V_1}$
		$v^*_{BN}=\min(v_R,v_Y,v_B)$	$\mathbf{V_5}$

5.4. Mitigation of DC neutral unbalance

For mitigation of DC neutral unbalance, it must be seen if a second pivot vector is possible other than the nearest pivot vector for the given 3-phase reference. This can be determined using the conditions given in Table VII.

If two pivot vectors are possible, one of the two is selected based on the DC neutral unbalance as explained in section 3. This final pivot vector, $\mathbf{V_{PF}}$, is subtracted from the 3-phase reference to get the reference for the conceptual two-level inverter as shown in (8).

$$\left(v_R^*, v_Y^*, v_B^*\right) = \left(v_R, v_Y, v_B\right) - \left(v_{PFR}, v_{PFY}, v_{PFB}\right) \quad ...(8)$$

5.5. Calculation of dwell times and switching instants

The maximum and minimum values of (v_R^*, v_Y^*, v_B^*) are identified as shown in (9).

$$v_{MAX}^* = \max(v_R^*, v_Y^*, v_B^*)$$
$$v_{MIN}^* = \min(v_R^*, v_Y^*, v_B^*) \quad ...(9)$$

The middle value is designated as v_{MID}^*. We have,

$$v_{MIN}^* + v_{MID}^* + v_{MAX}^* = 0 \quad ...(10)$$

Let an offset voltage v_{OFF}^* be added as a zero-sequence component to $(v_{MAX}^*, v_{MID}^*, v_{MIN}^*)$ to ensure that the dwell time for the pivot vector is equally divided between the two pivot states.

$$\left(v_{MAX}^{**}, v_{MID}^{**}, v_{MIN}^{**}\right) = \left(v_{MAX}^*, v_{MID}^*, v_{MIN}^*\right) + \left(v_{OFF}^*, v_{OFF}^*, v_{OFF}^*\right) \quad ...(11)$$

One pivot state is applied at the start of the subcycle, while the other is applied at the end. Considering the peak of the triangular carrier to be 0.5 and if both pivot states are to be applied for an equal duration of time, then

$$0.5 - v_{MAX}^{**} = v_{MIN}^{**} - (-0.5)$$
$$\Rightarrow v_{MAX}^{**} + v_{MIN}^{**} = 0 \quad ...(12)$$

Substituting for v_{MAX}^{**} and v_{MIN}^{**} in (12) from (11), the offset voltage required can be calculated as shown in (13).

$$v_{MAX}^* + v_{MIN}^* + 2v_{OFF}^* = 0$$
$$\Rightarrow v_{OFF}^* = -\frac{(v_{MAX}^* + v_{MIN}^*)}{2} = -\frac{v_{MID}^*}{2} \quad ...(13)$$

The offset voltage, added as a zero-sequence component to (v_R^*, v_Y^*, v_B^*), yields the modified three-phase reference for the conceptual two-level inverter $(v_R^{**}, v_Y^{**}, v_B^{**})$ as shown in (14). The switching instants for the three phases are available from $(v_R^{**}, v_Y^{**}, v_B^{**})$.

$$\left(v_R^{**}, v_Y^{**}, v_B^{**}\right) = \left(v_R^*, v_Y^*, v_B^*\right) + \left(v_{OFF}^*, v_{OFF}^*, v_{OFF}^*\right) \quad ...(14)$$

The two-level PWM from $(v_R^{**}, v_Y^{**}, v_B^{**})$ can be translated into 3-level PWM waveform using the final pivot vector as shown in Table VIII.

TABLE VIII: TWO-LEVEL TO THREE-LEVEL PWM

Final pivot vector	R-phase			Y-phase			B-phase		
	2-level PWM	S1	S4	2-level PWM	S1	S4	2-level PWM	S1	S4
$\mathbf{V_1}$	HIGH	ON	OFF	HIGH	OFF	OFF	HIGH	ON	OFF
	LOW	OFF	OFF	LOW	OFF	ON	LOW	OFF	OFF
$\mathbf{V_2}$	HIGH	ON	OFF	HIGH	OFF	OFF	HIGH	OFF	OFF
	LOW	OFF	OFF	LOW	OFF	ON	LOW	OFF	ON
$\mathbf{V_3}$	HIGH	ON	OFF	HIGH	ON	OFF	HIGH	OFF	OFF
	LOW	OFF	OFF	LOW	OFF	OFF	LOW	OFF	ON
$\mathbf{V_4}$	HIGH	OFF	OFF	HIGH	ON	OFF	HIGH	OFF	OFF
	LOW	OFF	ON	LOW	OFF	OFF	LOW	OFF	ON
$\mathbf{V_5}$	HIGH	OFF	OFF	HIGH	ON	OFF	HIGH	ON	OFF
	LOW	OFF	ON	LOW	OFF	OFF	LOW	OFF	OFF
$\mathbf{V_6}$	HIGH	OFF	OFF	HIGH	OFF	OFF	HIGH	ON	OFF
	LOW	OFF	ON	LOW	OFF	ON	LOW	OFF	OFF
	$S2 = \overline{S4},\ S3 = \overline{S1}$			$S2 = \overline{S4},\ S3 = \overline{S1}$			$S2 = \overline{S4},\ S3 = \overline{S1}$		

6. Proposed PWM algorithm

Based on the discussions in the earlier section, the proposed algorithm is summarized in this section.

1. Identify the nearest pivot vector, $\mathbf{V_{PN}}$, using (v_R, v_Y, v_B) as shown in Table VII.
2. Calculate $(v_{RN}^*, v_{YN}^*, v_{BN}^*)$ using (v_R, v_Y, v_B) and $\mathbf{V_{PN}}$ as given in (7).
3. Determine if a second pivot vector other than the nearest pivot vector is possible using $(v_{RN}^*, v_{YN}^*, v_{BN}^*)$ as shown in Table VII.
4. If two pivot vectors are possible, then select the final pivot vector, $\mathbf{V_{PF}}$, based on DC neutral

unbalance as explained in section 3. Otherwise the nearest pivot vector is the final pivot vector.

5. Calculate three-phase reference for the two-level inverter (v_R^*, v_Y^*, v_B^*) using (v_R, v_Y, v_B) and $\mathbf{V_{PF}}$ as shown in (8).

6. Identify the maximum, middle and minimum modulating waves for the two-level inverter $(v_{MAX}^*, v_{MID}^*, v_{MIN}^*)$ as indicated in (9) and (10).

7. Calculate offset voltage v_{OFF}^* using $(v_{MAX}^*, v_{MID}^*, v_{MIN}^*)$ as shown in (13).

8. Add v_{OFF}^* as a zero-sequence component to (v_R^*, v_Y^*, v_B^*) in order to obtain $(v_R^{**}, v_Y^{**}, v_B^{**})$, the modified three-phase reference for the conceptual two-level inverter as in (14).

9. Generate two-level PWM using $(v_R^{**}, v_Y^{**}, v_B^{**})$.

10. Translate the two-level PWM into three-level PWM using the current $\mathbf{V_{PF}}$ as indicated in Table VIII.

The algorithm is still simpler if mitigation of DC neutral voltage by change of pivot vector is not attempted.

7. Results

The simulation of the algorithm is done using MATLAB/SIMULINK. The modulating signals v_R, v_R^* and v_R^{**} are shown in dotted, dashed and solid lines, respectively, in Fig. 6 for maximum modulation index. The triangular carrier (not shown) has a peak of ± 0.5.

The proposed algorithm is implemented on a TMS320F240 based digital controller platform. It is tested on a 415V, 5hp, 50Hz, 3-phase induction motor drive fed from an IGBT-based 10kVA three-level inverter. Measured no-load current at the maximum modulation index is presented in Fig. 7.

8. Conclusion

A computationally efficient PWM algorithm has been proposed for three-level voltage source inverters. This algorithm is the result of a study on centred space vector PWM for multilevel inverters, and a systematic simplification of the same. The proposed algorithm does not involve three-phase to two-phase transformation, rectangular to polar coordinate transformation, or evaluation of any trigonometric function. The algorithm is tested through simulations as well as experimentally.

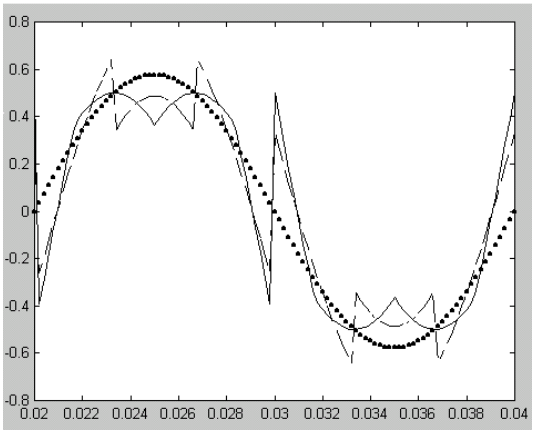

Fig. 6 v_R, v_R^* and v_R^{**} for maximum modulation index

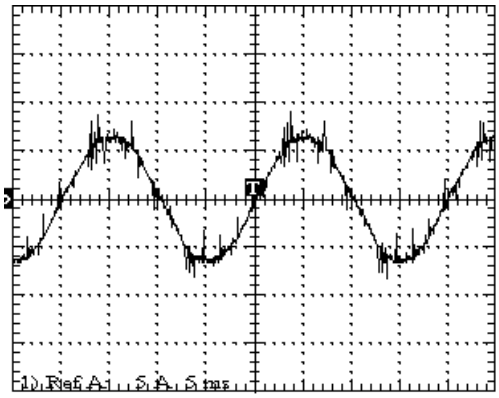

Fig. 7 Measured no-load current at maximum modulation index

References

[1] Y-H. Lee, B-S. Suh and D-S. Hyun, "A novel PWM scheme for a three-level voltage source inverter with GTO thyristors," IEEE Trans. IA, Vol. 32(2), pp. 260-268, Mar/Apr 1996.

[2] J. H. Seo, C. H. Choi and D. S. Hyun, "A new simplified space-vector PWM method for three-level inverters," IEEE Trans. PE, Vol. 16(4), pp. 545-550, July 2001.

[3] F. Wang, "Sine-triangle versus space-vector modulation for three-level PWM voltage-source inverters," IEEE Trans. IA, Vol. 38(2), pp 500-506, Mar/Apr 2002.